One Stone Three Birds: Regiodivergent Access to Amino-Substituted Benzophospholes and Their Structure–Property Relationships

Jiahao Zhu, Lili Wang, * and Zheng Duan *

College of Chemistry, Green Catalysis Center, International Phosphorus Laboratory, International Joint Research Laboratory for Functional Organophosphorus Materials of Henan Province, Zhengzhou University, Zhengzhou 450001, China

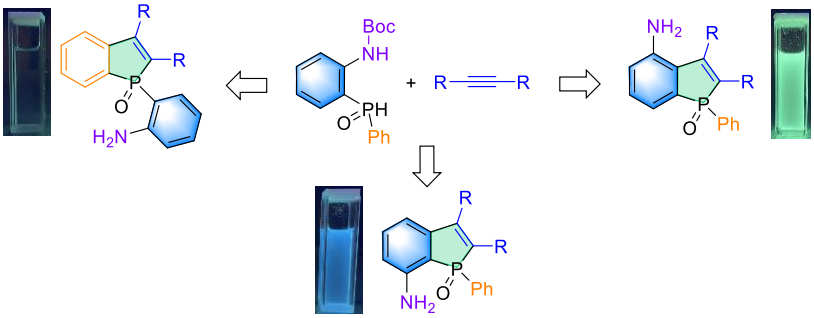

Abstract: Three series new NH_2-benzophosphole oxides were synthesized from cycloaddition of *o*-aminophenyl phosphine oxide with alkynes. Photophysics investigation and theoretical calculation indicate that the position of amino group in these benzophosphole oxides obviously regulate their properties. 4-NH_2-benzo[b]phosphole oxides show strong fluorescence emission and high fluorescence quantum efficiency. This "One stone three birds" process provides rapid access to multiple organophosphorus based luminogens for the structure–property relationship study.

Benzophosphole has received increasing research interest in the past decades for its unique optoelectronic features and potentially broad applications in material science.[1] The photoelectric properties of the annulated core can be tuned by substitution pattern and substitute group.[2] Recently, the incorporation of amino groups to form donor-acceptor-type luminogens attracts considerable attention. For example, Yamaguchi's group reported an arylamine group attached benzophosphole (Ⅰ), which was polarity-sensitive and used as an environment-sensitive fluorescent probe.[3] Tang's group investigated several benzophosphole oxides containing acridine (Ⅱ) or arylamine (Ⅲ) or pyridine groups as AIEgens for OLED or photodynamic therapy applications.[4] Yoshikai and co-workers introduced the amino group, with or without a π spacer at C5-position (Ⅳ), the compounds with a π spacer displayed stronger solvatochromism than those without a π spacer.[5]

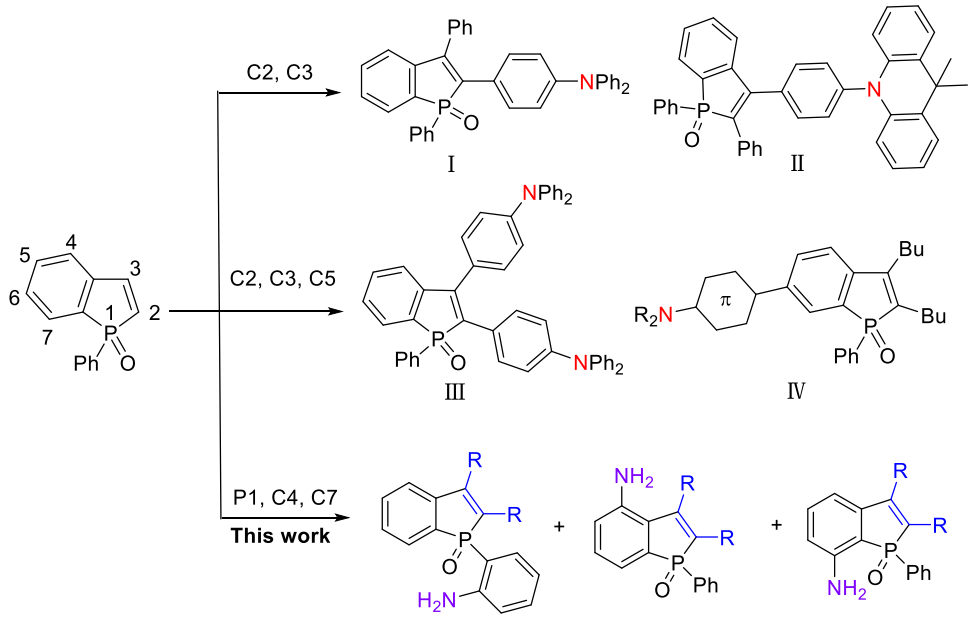

Figure 1 Structure of Benzophosphole and Some Representative Benzo[b]phospholes with Amino Groups

Miura, Satoh and their coworkers have reported an approach to benzophosphole oxides from intermolecular cyclization of alkynes and secondary phosphine oxides in the presence of AgOAc in DMF at 100 °C.[11] Following this avenue, we designed and synthesized an *ortho*-Boc-aminophenyl phosphine oxide **1**, which reacted with diphenylacetylene firstly. The reaction was monitored by ^{31}P NMR and three new phosphorus derivatives were observed in the resulting reaction mixture. These three products were isolated in pure form by simple column chromatography in a total 85% yield. Based on the NMR spectra, these three regioisomers differing in the location of amino group were recognized as **3a** (^{31}P NMR: δ = 47.9 ppm in $CDCl_3$, eluent: PE:EA = 5:1, R_f = 0.3, yield: 18%), **3b** (^{31}P NMR: δ = 38.0 ppm in $CDCl_3$, eluent: PE:EA = 1:1, R_f = 0.1, yield: 38%), and **3c** (^{31}P NMR: δ = 39.1 ppm in $CDCl_3$, eluent: PE:EA = 3:1, R_f = 0.2, yield: 29%). The ratio of **3b** in the total yield is high, which may be caused by the large steric hindrance of NHBoc group. This result was consistent with previous report and the plausible mechanism was proposed in ESI (Scheme S1).[12] Encouraged by these results, we started to examine the reaction scope. All the reactions proceed smoothly with good substrates tolerance. To our gratify, all of the isomers could be separated easily and the desired Boc-protected products **4a**~**7a**, **4b**~**7b** and **4c**~**7c** were obtained in medium overall yields (37%~62%) (Scheme 1A). In the presence of trifluoroacetic acid (TFA), the Boc-protected products **3a**~**7a**, **3b**~**7b** and **3c**~**7c** were converted into the corresponding NH_2-substituted products **3a'**~**7a' (a'** series**)**, **3b'**~**7b' (b'** series**)** and **3c'**~**7c' (c'** series**)** in 52%~93% yields (Scheme 1B). These products were identified by NMR spectra, high-resolution mass spectrometry, and X-ray crystallographic analysis of **3b'** (CCDC 2161224) and **7c'** (CCDC 2161185), respectively (Figure 2).

Scheme 1 Synthesis of three regioisomers NH_2-Substituted benzo[b]phosphole oxides[a]

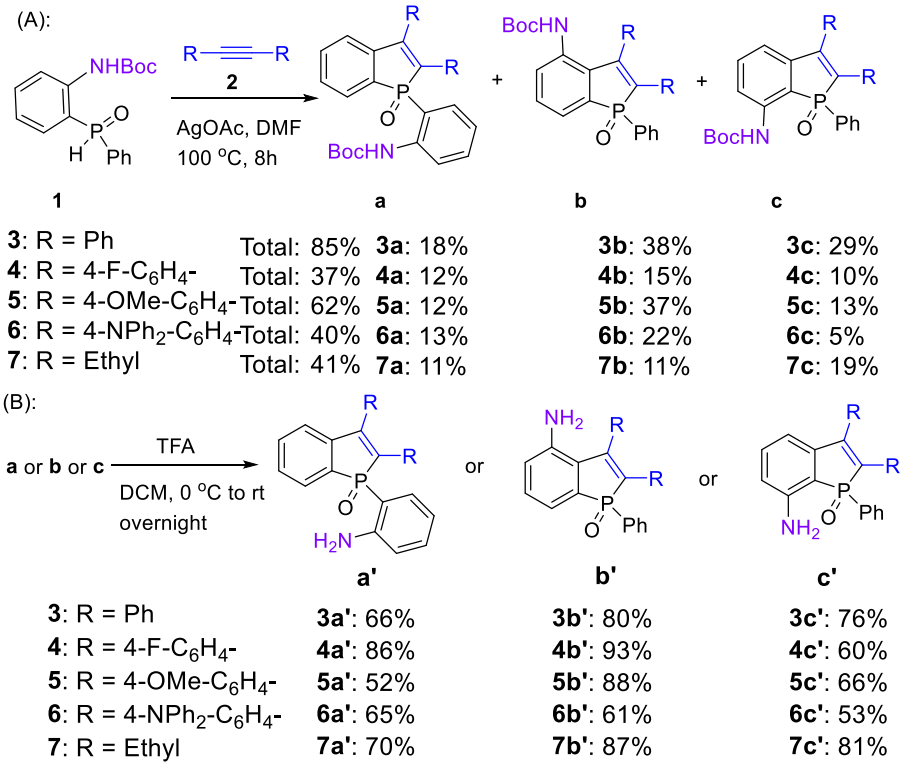

[a]Reaction conditions: (A) **1** (1.0 mmol), **2** (0.5 mmol), AgOAc (2 mmol), DMF (3.0 mL), under N_2 atmosphere. All yields were isolated and based on substrate **2**. (B) **a** (**b**, **c**) (0.2 mmol), TFA (0.6 mL), DCM (1.0 mL). All yields were isolated and based on substrate **a** (**b**, **c**).

The crystal analysis revealed a π-π stacking interaction between the two adjacent benzophosphole cores of **3b'** with a distance of 3.528 Å (Figure 2). Water molecules were observed within the crystal, which formed two types of hydrogen bonds: P=O···H-OH and H_2O···H-NH with distances of 1.914 Å and 2.084 Å, respectively in **3b'**. There were also intermolecular hydrogen bonds P=O···H-NH with a distance of 2.517 Å in **7c'**. Additionally, C-H···π interaction was found between C4-H and benzophosphole core (2.744 Å) in **7c'**. Due to the presence of amino groups, supramolecular structures are formed through hydrogen bonds and π-π interactions in the solid **3b'** and **7c'**, respectively.

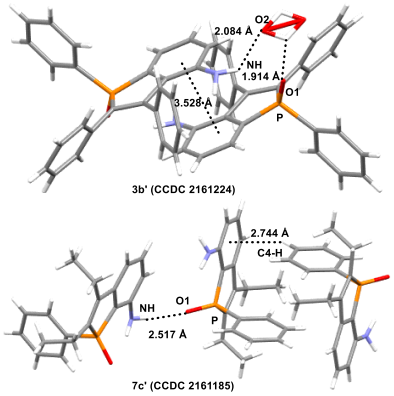

Figure 2. X-ray crystal structures of **3b'** and **7c'** with the packing view

These structurally simple regioisomers differing in the location of NH_2 group were analyzed by UV-Vis absorption and fluorescence emission. As shown in Table 1 and Figure 3, the location of NH_2 group has a significant impact on the optical properties. Except of the strong electron-donating diphenylamino substituted **6**, the λ_{max} and λ_{em} of 4-NH_2-benzophosphole (**b'** series) > 7-NH_2-benzophosphole (**c'** series) > 1-(2'-NH_2-phenyl)-benzophosphole (**a'** series). Series **b'** exhibited strong fluorescence emission and showed the highest fluorescence quantum yields. In contrast, weak or even no luminescence was seen from **a'** series. Compared with **TPPIO** (Figure 3, λ_{max} = 340 nm and λ_{em} = 426 nm), **3a'** (λ_{max} = 338 nm and λ_{em} = 388 nm) is blue shifted.[13] There are red shifts in absorption and emission as NH_2 group anchored on the annulated phenyl ring, larger shifts were displayed in **3b'** (λ_{max}= 396 nm and λ_{em}= 499 nm) than those of **3c'** (λ_{max} = 362 nm and λ_{em} = 458 nm). Similar trends were observed in **4a'**~**4c', 5a'**~**5c',** and **7a'**~**7c'** also (See Figure S1 in ESI). However, the difference between λ_{em} of **6a'**~**6c'** is smaller, while **6a'** has the most red-shifted λ_{em} (565 nm). Contrasted with **$(TPA)_2$PIO** (Figure 3) the emission wavelengths of **6a'**~**6c'** are slightly red-shifted.[4a]

Table 1 Photophysical Data of the Products[a]

Entry	Compound	λ_{max}(nm)[a]	λ_{em}(nm)[b]	Φ_f(%)[c]
1	**3a'**	338	388	0
2	**3b'**	396	499	29
3	**3c'**	362	458	6
4	**4a'**	338	403	0
5	**4b'**	396	495	52
6	**4c'**	361	457	7
7	**5a'**	371	398	1
8	**5b'**	401	500	72
9	**5c'**	372	492	4
10	**6a'**	395	565	34
11	**6b'**	428	548	45
12	**6c'**	397	556	37
13	**7a'**	322	388	0
14	**7b'**	365	447	9
15	**7c'**	350	410	27
16[12]	**TPPIO**	340	426	3
17[4a]	**$(TPA)_2$PIO**[d]	410	543	44

[a]Measured in DCM. [b] Emission maxima upon excitation at the absorption maximum wavelengths. [c]Relative fluorescence quantum yield in DCM, relative to quinine sulfate (H_2SO_4, 0.1 M solution). [d]Measured in THF. Definitions: λ_{abs}, longest wavelength absorption maxima; λ_{em}, emission maxima; Φ_f, fluorescence quantum yield.

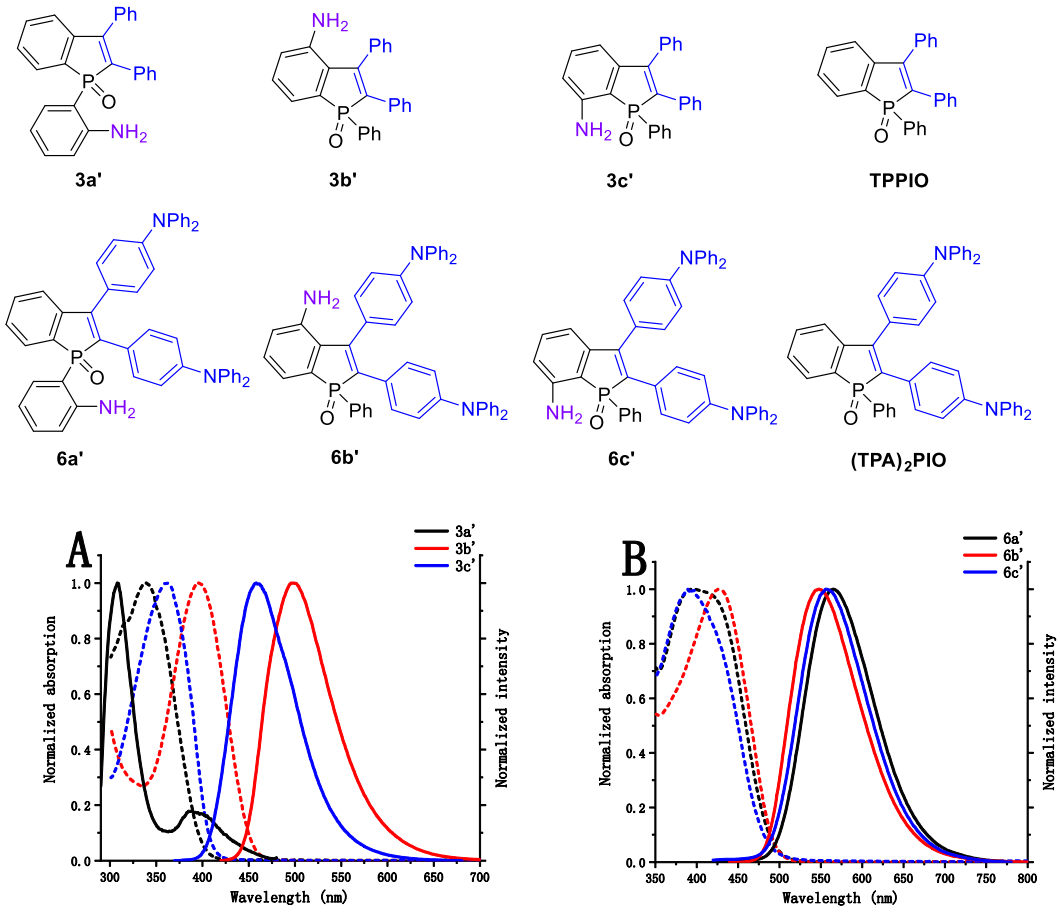

Figure 3. Chemical structures of **3**, **TPPIO**, **6** and **(TPA)$_2$PIO**, UV/Vis absorption (dashed lines) and normalized emission (solid lines) spectra of compounds **3** (A) and **6** (B) in CH_2Cl_2 at 298 K

In order to further understand the relationship between the structure and optical behaviors of these luminogens, electronic structures of **3a'**~**3c'** and **6a'**~**6c'** were calculated using density functional theory at the basis set level of B3LYP/6-31+ G(d, p). As illustrated in Figure 4, the introduction of NH_2 group has greatly changed the distribution of HOMO in **3a'**~**3c'**. The HOMO orbital of **3a'** is mainly distributed on the peripheral aminophenyl with very limited delocalization size. Compared with **TPPIO**,[13] the presence of NH_2 group changed the shape and size of HOMO. HOMOs of **3b'** and **3c'** are well delocalized across NH_2 group and benzophosphole core, while the contribution from phenyl at C4-position decreases dramatically. The LUMO orbital distributions of **3a'**~**3c'** are similar, mainly concentrated on benzophosphole core and two phenyls at 2 and 3-positions. **6a'**~**6c'** have similar LUMO distributions, which are mainly localized on benzophosphole core and the phenyl at 2-position. The diphenylamino moieties of **6a'** and **6c'** influence the HOMO predominantly while the contribution from NH_2 moiety is negligible. However, **6b'** has well-delocalized HOMO along the long molecular axis with the involvement of NH_2 moiety, benzophosphole core, and diphenylamine at 2-position. This computational calculation confirmed a larger contribution from benzophosphole core to HOMO of **6a'**~**6c'** than **(TPA)$_2$PIO**.[4a] These results clearly showed that NH_2 groups anchored on the annulated phenyl ring of benzophosphole

core can effectively affect their photophysical properties, and the photophysical properties of **6a'~6c'** are controlled by their triphenylamine substitutes.

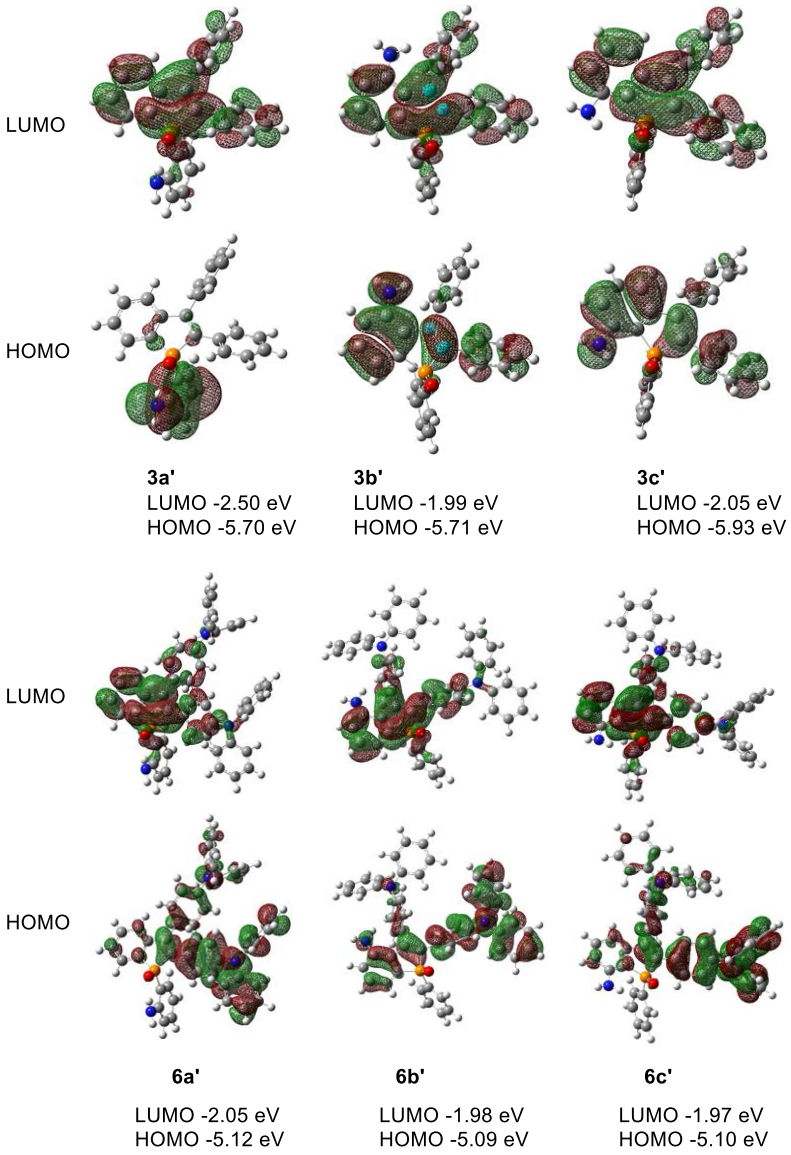

Figure 4. Frontier orbitals of **3** and **6**

Subsequently, we studied the effect of 2,3-substituents on the optical properties. As shown in Table 2 and Figure 3, all of the electron neutral **3b'** (λ_{max} = 396 nm and λ_{em} = 499 nm), electron-withdrawing fluoride substituted **4b'** (λ_{max} = 396 nm and λ_{em} = 495 nm), and electron-donating OMe substituted **5b'** (λ_{max} = 401 nm and λ_{em} = 500 nm) have similar UV-vis absorption and emission peaks. **6b'** (λ_{max} = 428 nm and λ_{em} = 548 nm) showed significantly red-shifted absorption and emission. In comparison, the ethyl substituted **7b'** (λ_{max} = 365 nm and λ_{em} = 447 nm) showed blue-shifted due to the reduced π-conjugation. 4-NH_2-substituted benzophospholes **3b'~7b'** displayed the best fluorescence quantum yields among three regioisomers, except alkyl-substituted **7b'**. The highest quantum yield was obtained with **5b'** (Φ_f = 72%). The UV-vis absorption and emission spectra of compounds **3a'~7a'** and **3c'~7c'** have the same trend as **3b'~7b'** (See Figure S2 in ESI).

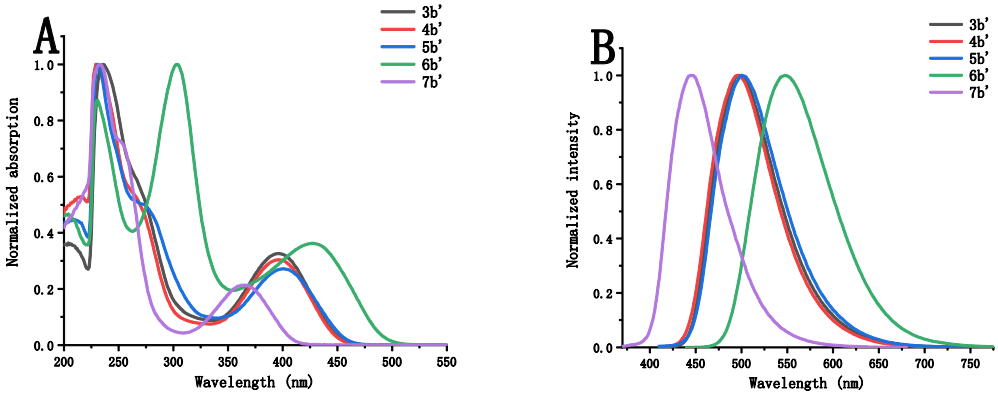

Figure 5 UV/Vis absorption (**A**) and normalized emission (**B**) spectra of compounds **3b'~7b'** (CH_2Cl_2, 298 K)

Table 2 Photophysical Data of **3b'** in Different Solvents[a]

Entry	Solvent	λ_{max}(nm)[a]	λ_{em}(nm)[b]	ε[10^4 M^{-1} cm^{-1}]	Φ_f[c](%)
1	Hexane	382	465	0.41	36
2	Toluene	391	493	1.26	-
3	DCM	396	499	0.99	29
4	THF	402	501	1.04	-
5	Acetone	401	507	1.08	-
6	DMF	408	516	0.99	-
7	DMSO	410	526	0.80	40

[a]Measured in solvent (1×10^{-5} M). [b]Emission maxima upon excitation at the absorption maximum wavelengths. [c]Relative fluorescence quantum yield in solvent, relative to quinine sulfate (H_2SO_4, 0.1 M solution).

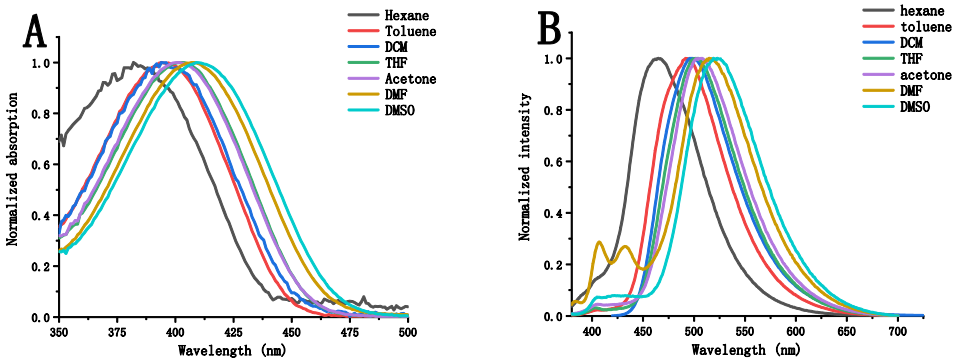

Figure 6. UV/Vis absorption (**A**) and normalized emission (**B**) spectra of compound **3b'** in different solvents (298 K)

The solvatochromism was studied with **3b'**, and it was found that the absorption and fluorescence spectra were both red-shifted gradually with the increased solvent polarity (Figure 6, Table 2). It should be pointed out that **3b'** is highly fluorescent (Table 2, entry 7) with a pronounced emission solvatochromism, which suggests the formation of an intramolecular charge-separated emitting state in DMSO. **3b'** has the largest molar absorption coefficient ε in toluene (Table 2, entry 2).

In summary, photophysics investigation and theoretical calculation of these structurally diverse isomers clearly indicated that the introduction and location of amino groups in these benzophosphole oxides obviously affect their photophysical properties. Among the three isomers, 4-NH_2-substituted derivatives exhibited the best emission performance. This research provides a new perspective and method for the structural engineering of benzophosphole, and the utilization and derivatization of the NH_2 group are in progress in our laboratory.

Supporting Information

Experimental procedures, characterization data for all new compounds including ^{1}H, ^{31}P, and ^{13}C NMR spectra, and Crystallographic data for **3b'** (CCDC 2161224) and **7c'** (CCDC 2161185).

Notes

The authors declare no competing financial interest.

Corresponding Authors

Lili Wang − College of Chemistry, Green Catalysis Center, International Phosphorus Laboratory, International Joint Research Laboratory for Functional Organophosphorus Materials of Henan Province, Zhengzhou University, Zhengzhou 450001, P. R. China; orcid.org/ 0000-0002-7411-8357; Email: wanglili@zzu.edu.cn

Zheng Duan − College of Chemistry, Green Catalysis Center, International Phosphorus Laboratory, International Joint Research Laboratory for Functional Organophosphorus Materials of Henan Province, Zhengzhou University, Zhengzhou 450001, P. R. China; orcid.org/0000-0002-0173-663X; Email: duanzheng@zzu.edu.cn

Author

Jiahao Zhu − College of Chemistry, Green Catalysis Center, International Phosphorus Laboratory, International Joint Research Laboratory for Functional Organophosphorus Materials of Henan Province, Zhengzhou University, Zhengzhou 450001, P. R. China

ACKNOWLEDGMENT

We are grateful for financial support from the National Natural Science Foundation of China (Nos. 22171245, 22101262, 21672193), the Key Scientific and Technological Project of Henan Province (No. 202102310327) and Zhengzhou University of China.

REFERENCES

(1) (a) Baumgartner, T.; Réau, R. Organophosphorus π-conjugated materials. *Chem. Rev.* **2006**, *106*, 4681-4727. (b) Matano, Y.; Imahori. H. Design and synthesis of phosphole-based π systems for novel organic materials. *Org. Biomol. Chem.* **2009**, *7*, 1258-1271. (c) Baumgartner, T. Insights on the design and electron-acceptor properties of conjugated organophosphorus materials. *Acc. Chem. Res.* **2014**, *47*, 1613-1622. (d) Duffy, M. P.; Delaunay, W.; Bouit, P. A.; Hissler, M. π-Conjugated phospholes and their incorporation into devices: components with a great deal of potential. *Chem. Soc. Rev.* **2016**, *45*, 5296-5310. (e) Joly, D.; Bouit, P. A.; Hissler, M. Organophosphorus derivatives for electronic devices. *J. Mater. Chem. C.* **2016**, *4*, 3686-3698. (f) Shameem, M. A.; Orthaber, A. Organophosphorus compounds in organic electronics. *Chem. Eur. J.* **2016**, *22*, 10718-10735.

(2) (a) Hissler, M.; Dyer, P. W.; Réau. R. Linear organic π-conjugated systems featuring the heavy group 14 and 15 elements. *Coord. Chem. Rev.* **2003**, *244*, 1-44. (b) Matano, Y. Synthesis and Structure-Property Relationships of Phosphole-Based π Systems and Their Applications in Organic Solar Cells. *Chem. Rec.* **2015**, *15*, 636-650. (c) Stolar, M.; Baumgartner, T. Phosphorus-Containing Materials for Organic Electronics. *Chem. Asian J.* **2014**, *9*, 1212-1225. (d) Nishida, J.; Kawakami, Y.; Yamamoto, S.; Matsui, Y.; Ikeda, H.; Hirao, Y.; Kawase, T. Synthesis and Photophysical Studies of Dibenzophosphole Oxides with D-A-D Triad Structures. *Eur. J. Org. Chem.* **2019**, *2019*, 3735-3743. (e) Zhong, D. K.; Yu, Y.; Song D. D.; Yang, X. L.; Zhang, Y. D.; Chen, X.; Zhou, G. J.; Wu, Z. X. Organic emitters with a rigid 9-phenyl-9-phosphafluorene oxide moiety as the acceptor and their thermally activated delayed fluorescence behavior. *ACS Appl. Mater. Interfaces.* **2019**, *11*, 27112-27124.

(3) Yamaguchi, E.; Wang, C. G.; Fukazawa, A.; Taki, M.; Sato, Y.; Sasaki, T.; Ueda, M.; Sasaki, N.; Higashiyama, T.; Yamaguchi, S. Environment-sensitive fluorescent probe: A benzophosphole oxide with an electron-donating substituent. *Angew. Chem. Int. Ed.* **2015**, *54*, 4539-4543.

(4) (a) Zhuang, Z. Y.; Bu, F.; Luo, W. W.; Peng, H. R.; Chen, S. M.; Hu, R. R.; Qin, A. J.; Zhao, Z. J.; Tang, B. Z. Steric, conjugation and electronic impacts on the photoluminescence and electroluminescence properties of luminogens based on phosphindole oxide. *J. Mater. Chem. C.* **2017**, *5*, 1836-1842. (b) Li, J. Q.; Zhuang, Z. Y.; Zhu, X. Y.; Zhao, Z. J.; Tang, B. Z. 9, 9-Dimethyl-9, 10-dihydroacridine functionalized phosphoindole oxides with AIE property for OLED application. *J. Inform Display.* **2020**, *21*, 139-147. (c) Zhuang, Z. Y.; Dai, J.; Yu, M. X.; Li, J. Q.; Shen, P. C.; Hu, R.; Lou, X. D.; Zhao, Z. J.; Tang, B. Z. Type I photosensitizers based on phosphindole oxide for photodynamic therapy: apoptosis and autophagy induced by endoplasmic reticulum stress. *Chem. Sci.* **2020**, *11*, 3405-3417.

(5) Yoshikai, N.; Santra, M.; Wu, B. Synthesis of Donor-Acceptor-Type Benzo[b]phosphole and Naphtho [2, 3-b] phosphole Oxides and Their Solvatochromic Properties. *Organometallics* **2017**, *36*, 2637-2645.

(6) (a) Afanasyev, O. I.; Kuchuk, E.; Usanov, D. L.; Chusov, D. Reductive amination in the synthesis of pharmaceuticals. *Chem. Rev.* **2019**, *119*, 11857-11911. (b) Campos, K. R.; Coleman, P. J.; Alvarez, J. C.; Dreher, S. D.; Garbaccio, R. M.; Terrett, N. K.; Tillyer, R. D.; Truppo, M. D.; Parmee, E. R. The Importance of Synthetic Chemistry in thePharmaceutical Industry. *Science* **2019**, *363*, eaat0805. (c) Skoda, E. M.; Davis, G. C.; Wipf, P. Allylic amines as key building blocks in the synthesis of (E)-alkene peptide isosteres. *Org. Process Res. Dev.* **2012**, *16*, 26-34. (d) Nicastri, M. C.; Lehnherr, D.; Lam, Y. H.; DiRocco, D. A.; Rovis, T. Synthesis of sterically hindered primary amines by concurrent tandem photoredox catalysis. *J. Am. Chem. Soc.* **2020**, *142*, 987-998. (e) Shao, Q.; He, J.; Wu, Q. F.; Yu, J. Q. Ligand-enabled γ-C (sp^3)-H cross-coupling of nosyl-protected amines with aryl-and alkylboron reagents. *ACS Catal.* **2017**, *7*, 7777-7782. (f) Liu, B.; Romine, A. M.; Rubel, C.

Z.; Engle, K. M.; Shi, B. F. Transition-Metal-Catalyzed, Coordination-Assisted Functionalization of Nonactivated C (sp^3)-H Bonds. *Chem. Rev.* **2021**, *121*, 14957-15074.

(7) Kessler, C. Non-radioactive analysis of biomolecules. *J. Biotechnol.* **1994**, *35*, 165-189.

(8) Cornforth, J.; Cornforth, R. H.; Gray, R. T. Synthesis of substituted dibenzophospholes. Part 1. *J. Chem. Soc., Perkin Trans.* 1, **1982**, 2289-2297.

(9) Panichakul, D.; Mathey, F. Serendipitous Discovery of a Phosphirene-Phosphindole Rearrangement. *Organometallics* **2011**, *30*, 348-351.

(10) Slootweg, J. C.; Vlaar, M. J. M.; Vugts, D. J.; Eichelsheim, T.; Merhai, W.; Kanter, F. J. J. D.; Schakel, M.; Ehlers, A. W.; Lutz, M.; Spek, A. L.; Lammertsma, K. Methylene-Azaphosphirane as a Reactive Intermediate. *Chem. Eur. J.* **2005**, *11*, 4808-4818.

(11) (a) Unoh, Y.; Hirano, K..; Satoh, T.; Miura, M. An Approach to Benzophosphole Oxides through Silver-or Manganese-Mediated Dehydrogenative Annulation Involving C-C and C-P Bond Formation. *Angew. Chem. Int. Ed.* **2013**, *52*, 12975-12979.

(12) Chen, Y. R.; Duan, W. L. Silver-mediated oxidative C–H/P–H functionalization: an efficient route for the synthesis of benzo[b]phosphole oxides. *J. Am. Chem. Soc.* **2013**, *135*, 16754-16757.

(13) Bu, F.; Wang, E. J.; Peng, Q.; Hu, R. R.; Qin, A. J.; Zhao, Z. J.; Tang, B. Z. Structural and theoretical insights into the AIE attributes of phosphindole oxide: the balance between rigidity and flexibility. *Chem-Eur. J.* **2015**, *21*, 4440-4449.